J. exp. Biol. ***175****, 251–266 (1993)*
Printed in Great Britain © The Company of Biologists Limited 1993

BEATING OF CILIA OF SEA URCHIN EMBRYOS: A CRITICAL COMPARISON OF THE NORMAL AND REVERSED BEATING OF CILIA OF ISOLATED CELLS

YOSHIHIRO MOGAMI, SHIMA SEKIGUCHI and SHOJI A. BABA
Department of Biology, Ochanomizu University, Otsuka, Tokyo 112, Japan

Accepted 2 October 1992

Summary

Two different types of ciliary beating, normal and reversed, were analyzed on the same cilia on cells isolated from echinoplutei. Bends on the cilium in reversed beating were observed to increase in curvature during propagation in the effective stroke of the beat, whereas in normal beating, bends propagate with a constant curvature in both effective and recovery strokes. The proximal region of the cilium showed an almost identical oscillation of shear angle in both normal and reversed beating with respect to the time normalized to the average beat period, which was determined by the rotational movement of the cell body. In reversed beating, a common temporal profile generated at the proximal region was preserved in the oscillation over the length of the cilium. The local oscillations in normal beating, however, changed in temporal profile as seen from base to tip. The conversion of the temporal oscillatory profile from normal to reversed beating occurred in association with changes in the centre of the oscillation (static bias), whose difference increased with the distance from the base. The data indicate that the changes in bending pattern between normal and reversed beating of sea urchin embryo cilia are not due to changes in the initiation of the oscillation at the base, but largely to temporal and static changes in the pattern of propagation of the oscillatory activity.

Introduction

Beating of cilia and eukaryotic flagella occurs as a result of sliding displacement between axonemal doublet-microtubules. In order to execute a specific pattern of bend formation, which, depending on the various environments of individual organelles, is well specialized for the effective transport of the surrounding medium, there must be a mechanism controlling the sliding movement of the doublet-microtubules. Comparative approaches analyzing bend formation in different types of beat patterns provide information relevant to the control mechanism. Analyses of bend formation of flagella using mutants of *Chlamydomonas* with functionally defective motile components (Brokaw *et al.* 1982; Brokaw and Luck, 1985; Brokaw and Kamiya, 1987) and of voltage-controlled ciliary beating in ciliates (Machemer, 1986; Sugino and Machemer, 1988, 1990; Mogami and Machemer, 1991) have increased our knowledge about the properties of the mechanism underlying the dynamic control of sliding movement.

Cilia of sea urchin embryos are a useful tool for a comparative study of ciliary bend

Key words: ciliary beating, angular oscillation, embryo cilia, sea urchin, *Hemicentrotus pulcherrimus.*

formation. The cilia change their type of response during the course of development, responding to electrical (Baba, 1975; Baba and Mogami, 1987) and Ca^{2+} stimulation (Degawa *et al.* 1986). Because the bend remained planar during the response, the bending transient could be analyzed with high time resolution (Baba and Mogami, 1987). In addition, an examination of the morphology of just a single cilium per cell made it possible to analyze the bend forms with high space resolution (Baba and Mogami, 1985).

In this paper, we focus on the reversal response of the cilia of pluteus larvae. Isolated cells from the ciliated epithelia rotate under the influence of their own ciliary movement with a beat plane constrained to be parallel to the surface of the microscope slide. Ciliated cells from pluteus larvae spontaneously change the net direction of rotation as a result of reversal of the beating direction. Reversed beating occurs with a different configuration from that of normal beating. This suggests that the regulation of the motile apparatus differs in normal and in reversed beating. We compared reversed beating with normal beating of the same cilium on a rotating cell, and characterized the difference between the two types of beating in terms of the temporal and spatial properties of local oscillatory activity along the length of the cilium.

Materials and methods

Isolation of ciliated cells from sea urchin embryos

Eggs and sperm of the sea urchin, *Hemicentrotus pulcherrimus*, were obtained by injection with 0.55mol l^{-1} KCl. Eggs were fertilized in Jamarin U artificial sea water (ASW, Jamarin Laboratory, Osaka) and developed at 17°C with paddle stirring (Degawa *et al.* 1986).

Pluteus larvae (40–60h after insemination) were collected by hand centrifuge and suspended in a dispersion medium (0.9mol l^{-1} glycine, 90mmol l^{-1} KCl, 2mmol l^{-1} EDTA, pH8.0). After 15min incubation at room temperature, the embryos became deformed and a few ciliated cells were dissociated by their own ciliary movement. To encourage dissociation, the suspension of embryos was pipetted in and out of a large-bore pipette (>3mm inner diameter). Aggregated cells, mainly of endodermal origin, and spicules were removed by low-speed centrifuge. Isolated cells in a dispersion medium were spun down and washed twice with Ca^{2+}-free ASW (465mmol l^{-1} NaCl, 10mmol l^{-1} KCl, 25mmol l^{-1} $MgCl_2$, 28mmol l^{-1} $MgSO_4$, 10mmol l^{-1} Tris–HCl, pH8.0) and suspended in the same medium. Cells were kept in suspension before use.

Before recording the ciliary movement, ASW containing an appropriate amount of $CaCl_2$ was added to produce a final composition in the medium of 450mmol l^{-1} NaCl, 10mmol l^{-1} KCl, 25mmol l^{-1} $MgCl_2$, 28mmol l^{-1} $MgSO_4$, 10mmol l^{-1} $CaCl_2$, 10mmol l^{-1} Tris–HCl, pH8.0 (standard ASW). A drop of the suspension was plated on the slide and covered with a coverslip using a 50 μm plastic film as a spacer. To allow cells to move freely, the glass surface was coated with agarose gel by flowing 0.05% hot agarose solution on its tilted upper surface, followed by air-drying.

Light microscopy

The movement of the ciliated cells was observed through a microscope (BH-2,

Olympus Optical Co., Tokyo) with phase-contrast optics (objectives, ×40NH, N/A 0.70) under stroboscopic illumination from a xenon flash tube (Strobex system 236, Chadwick-Helmuth, El Monte, CA). The movement was recorded by focusing the microscopic images through an ocular (×5FK, Olympus) and a 13-mm slit on 35-mm films (Plus-X or Tri-X, Eastman Kodak) with an oscilloscope camera (PC-2B, Nihon Koden, Tokyo) in running film mode at a film speed of $1\,\mathrm{m\,s^{-1}}$ and a stroboscope flash rate of 80Hz.

Data processing

We selected from the recordings images of cilia showing spontaneous reversed beating and normal beating recorded just before the response. Images that corresponded to the transition between normal and reversed beating were excluded (Baba and Mogami, 1987). Almost equal numbers of images of normal and reversed beating were used for the analysis of the movement.

Recorded films were enlarged with a microfilm reader to a final magnification of ×4000. Direct photographic prints and tracings on the screen of the microfilm reader were used for the point by point analysis, where the coordinates of the ciliary shaft were measured along the length of the cilium at intervals of 0.2–0.3 μm on a digitizer (Gradimate U4-30, Oscon Co., Tokyo) interfaced with a minicomputer (OKITAC 50/10, Oki Elec. Ind. Co., Tokyo).

For the assessment of rotational movement of ciliated cells, the orientation of the cell, which was defined by a vector directed from the centre of the cell (the centre of rotation) to the base of the cilium, was measured using fixed geometrical markers in the focal field. Parameters of the rotational movement were obtained by fitting analytical equations to the data (see Results) by the method of least squares for non-linear functions (Powell, 1965), using a program written by Dr Y. Oyanagi and filed in the library ($C7/TCPOW_I$) of the Computer Center of the University of Tokyo.

Shear angles (i.e. tangential angles) of a cilium, as a function of distance along the cilium, were calculated following a method described previously (Baba and Mogami, 1985), using a smoothing parameter of n=6 (cf. Fig. 2 in Baba and Mogami, 1985). The method is briefly summarized as follows.

The radius of curvature $\Gamma_{j,j+n}$ of a circular arc passing through the points P_j and P_{j+n} was obtained by averaging the radii of two circular arcs defined by two sets of three points; P_{j-n}, P_j, P_{j+n} and P_j, P_{j+n}, P_{j+2n}. The mean value of the curvature γ_j of the cilium between P_j and P_{j+1} was then calculated by averaging $\Gamma_{j-n+1,\,j+1}$, $\Gamma_{j-n+2,\,j+2}$, ..., $\Gamma_{j,\,j+n}$. The arc length between P_j and P_{j+1} (Δs_j) was calculated using γ_j and the straight-line distance between the points. The length measured along the cilium (s_j) and shear angle (ϕ_j) at P_j were computed using:

$$s_j = \sum_{i=0}^{j-1} \Delta s_i$$

and

$$\phi_j = \sum_{i=0}^{j-1} \gamma_i \Delta s_i + \phi_0 ,$$

where ϕ_0 is a constant. In the present study ϕ_0 is set at 0, so that shear angle is represented as the deviation (positive in the direction of the effective stroke of normal beating) from the normal to the cell surface at the base of the cilium.

In order to reduce noise due to errors of digitization, resultant shear curves were smoothed once by a method of moving averages on linear functions (SG13, in the library supplied by Oki Elec Ind. Co.); smoothed values for each data point were calculated by linear regression of the point and its nearest neighbours on both sides. Ciliary bending shapes shown in this paper were drawn by computer, utilizing the smoothed values. For the analysis of local oscillatory activity of the cilium, shear angles at a given distance from the base were calculated by interpolation from the data set of the shear curves, and were plotted as a function of the percentage of the beat period, which was determined by the analysis of the rotational movement of the cell. The mean course of the plot (curves in Fig. 5A) was determined by the smoothing method described above. The amplitude and centre of the oscillation were calculated from the maximum and minimum values found in the mean course.

Results

Rotational movement of isolated cells

Isolated cells were observed to rotate on the slide surface by their own ciliary movement (Fig. 1). The rotation was observed to occur around a fixed point, with little translocation of the cell body parallel to the surface. While the cell rotated steadily, ciliary beating occurred parallel to the slide surface. Since embryonic cilia show a planar bend configuration (Baba, 1975; Baba and Mogami, 1987), we can observe the whole length of the cilium in the same focal plane (Fig. 1). The planar bend configuration was further confirmed by recording with an objective of higher numerical aperture (1.25, ×100NH, Olympus).

Cells rotated with a back-and-forth movement, which depended on the alternately reversing force generation corresponding to the effective and recovery strokes of the beat (Figs 1 and 2A,B). The net direction of the rotation was constant in Ca^{2+}-free ASW and changed spontaneously in standard ASW containing Ca^{2+}. It was observed that steady rotation was often interrupted by reversals of the rotational direction usually lasting for several hundred milliseconds. Because there is a single cilium per cell, changes in the net direction of cell rotation should correspond to a change in the effective direction of water transport generated by the cilium. In the present study, we compared the ciliary movements recorded from cells that spontaneously changed their net direction of rotation.

Fig. 2A,B shows the time course of the changes in cell orientation recorded from the same cell. As shown in the insets of the figure, this change in the net direction of the cell rotation was associated with an alteration in the beat pattern, with the effective stroke reversing in direction. In this paper, the rotational motion caused by the effective and recovery strokes of normal beating are called E-rotation (clockwise in Fig. 1) and R-rotation (counterclockwise in Fig. 1), respectively. In the rotational movement performed

during normal beating, transitions between E- and R-rotations appeared to occur gradually (Fig. 2A), whereas, in the rotational movement caused by reversed beating, the transition from E- to R-rotation occurred rather abruptly (Fig. 2B). In order to

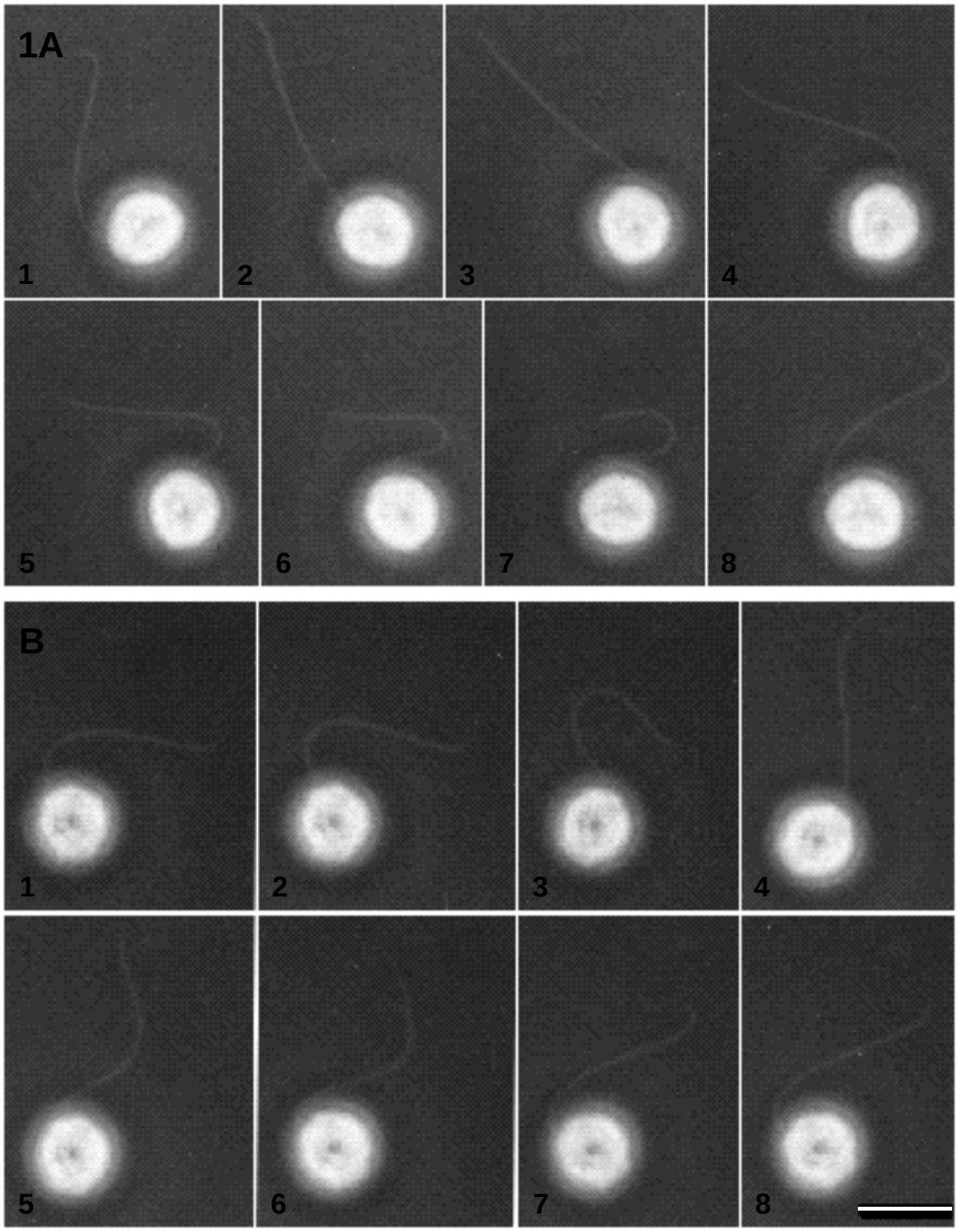

Fig. 1. Sequential photomicrographs of normal (A) and reversed (B) beating recorded from the same cell. Each frame is arbitrarily numbered following the sequence recorded at intervals of 12.5ms. Note the back-and-forth movement of the cell influenced by the movement of the cilium. Scale bar, 10 μm.

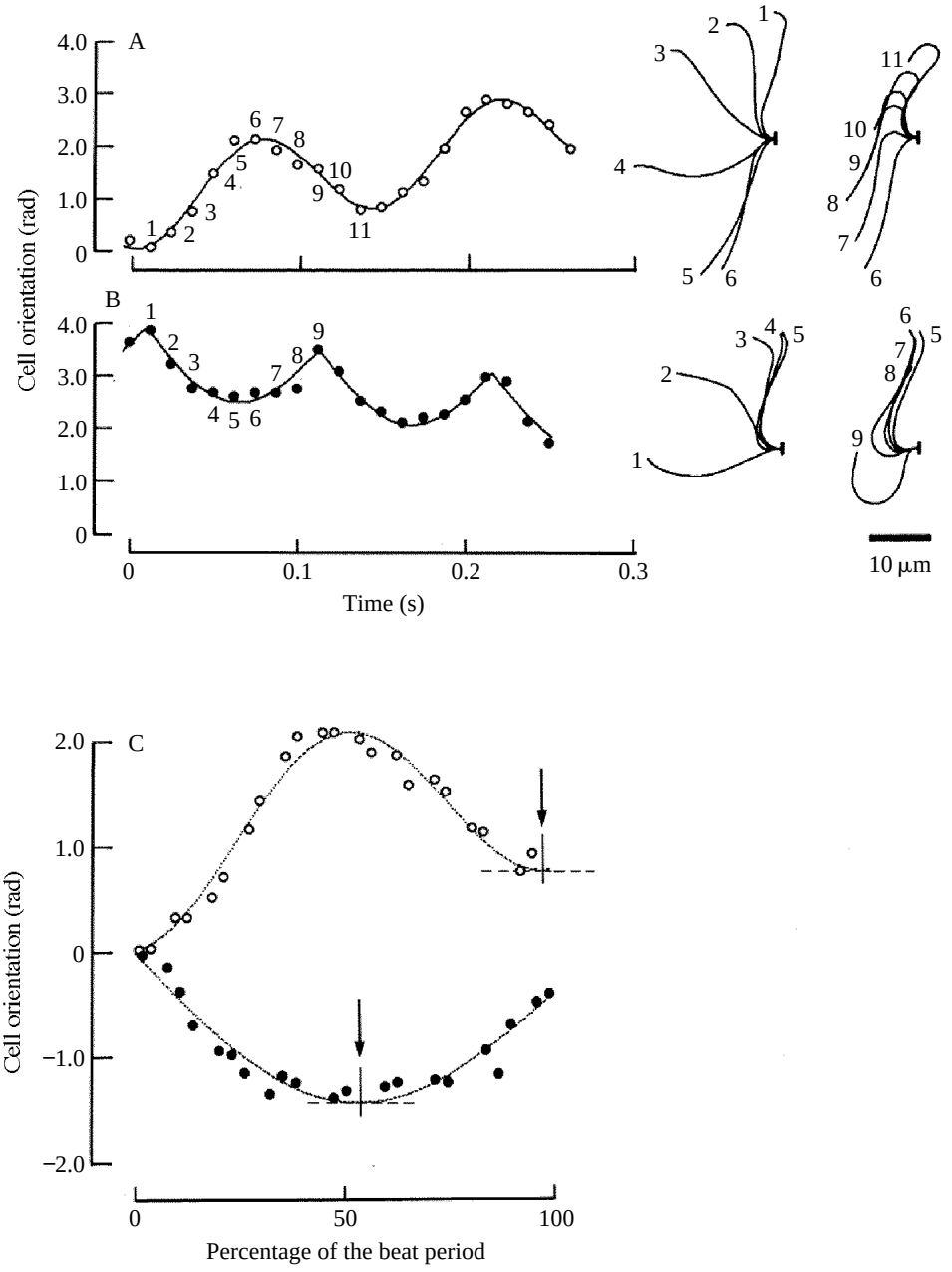

Fig. 2

characterize the rotational movement, which appeared to differ between normal and reversed beating, we fitted the data to two analytical equations:

$$\theta(t) = a + v_r t - \theta_r \cos 2\pi (t - b) f_r , \quad (1)$$

Fig. 2. (A,B) Time course of the rotational movement of the cell in normal (A) and reversed (B) beating. Measurements from the same cell are shown. Curves in A and B represent the results of least-squares fitting of equations 1 and 2, respectively. Insets show the bend configuration of the cilium at the time indicated by the numbers beside the curves. (C) Plot of the cell rotation in normal (open circles) and reversed beating (filled circles) as a function of the percentage of the beat period. The orientation *versus* time data (A and B) were divided into sets at intervals of one period of vibratory motion ($1/f_r$), and each data point is superimposed on one of the sets after subtracting the off-sets (*a* and *b*) and the average rotation for one beat characterized by v_r. Dotted lines indicate the curves fitted by least squares. Arrows in C indicate the beginning of E-rotation, defined as the transition point where derivatives of the fit functions change from negative to positive.

for normal beating, and:

$$\theta(t) = a + v_r t - \theta_r |\sin\pi(t-b)f_r| \quad (2)$$

for reversed beating (Fig. 2A,B). In equations 1 and 2, *a* and *b* are the spatial and temporal off-sets and v_r, θ_r and f_r are the mean rotation velocity, and amplitude and frequency of vibratory motion, respectively. In Fig. 2C, the functions (equations 1 and 2) are compared with the data points which were replotted within one cycle, after shifting using the parameters obtained by the least-squares fitting. Exchange of the equations between least-squares fitting for normal and reversed beating, i.e. fitting equation 2 to normal beating and equation 1 to reversed beating, significantly increased the root mean squares value, a measure of the goodness of fit, from 0.164±0.038rad (mean ± S.D., six cells) using equation 1 to 0.227±0.035rad using equation 2 for normal beating, and from 0.147±0.047rad (six cells) using equation 2 to 0.208±0.050rad using equation 1 for reversed beating. Table 1 shows parameters of the rotational movements fitted for six cells. In spite of the substantial increase in the root mean squares value, exchanging the equations caused only a small change in f_r (−0.6±0.7%, range −1.5 to 0.9%, mean ± S.D., six cells) and v_r (1.8±0.4%, range −3.2 to 10.3%). These data indicate that cilia generate propulsive thrust that is not identical in normal and reversed beating. Judging from the goodness of least-squares fitting, we used f_r obtained using equations 1 and 2 for

Table 1. *Parameters of rotational movement of isolated cells*

	Vibratory motion			
	Frequency (Hz)	Amplitude (rad)	Net angular velocity (radbeat^{-1})	*N*
Normal beating	10.7±2.9	0.91±0.09	0.71±0.13	6
	(10.6±2.8)	(1.03±0.10)	(0.72±0.15)	
Reversed beating	10.4±1.3	0.80±0.10*	0.50±0.10	6
	(10.2±1.4)	(0.66±0.08*)	(0.51±0.11)	

Values are mean ± S.D. obtained from identical cells by fitting equations 1 and 2 to normal (2–15 cycles) and reversed beating (2–13 cycles), respectively. Numbers in parentheses show values obtained by exchanging the equations fitted.

*$\theta_r/2$ obtained from fitting equation 2.

the analysis of bending motion in normal and reversed beating, respectively. Table 1 indicates that the net angular velocity of rotation is smaller in reversed beating than in normal beating.

Analysis of ciliary beating

Spontaneous reversed beating usually lasted for several hundred milliseconds. In such a short time, we observed only a few cycles of beating. In order to obtain an averaged bending motion, we reconstructed beating within one cycle by sorting the recorded images of different beat cycles by the percentage of the beat period. We used the value of f_r obtained from the least-squares fitting of the rotational movement of cell bodies to calculate the percentage value within the averaged beat period, defining the 'zero time' (0% of beat period) at the transition from R-rotation to E-rotation (Fig. 2C). Images were sorted in the same way for normal beating. Cells that continued reversed beating for more than two cycles were used for analyses.

Figs 3 and 4 show the shear curves of a cilium in normal and reversed beating, respectively. In these curves, descending limbs (regions between open circles) correspond to bends with their convex side towards the direction of the effective stroke of normal beating (E-bend) and ascending limbs (regions between filled circles) correspond to bends in the opposite direction (R-bend). The slope of the limb represents the curvature of the bend. In normal beating, both descending and ascending limbs retain an almost constant slope as they shift along the length of the cilium, indicating that both E- and R-bends propagate with constant curvatures (Fig. 3). In reversed beating, in contrast, such constancy of curvature was observed only during the propagation of the E-bend. Fig. 4 shows that the R-bend of reversed beating gradually increased in curvature during tipward propagation, reaching a similar value to that of the R-bend of normal beating. The increment of curvature during the propagation of the R-bend was found in all recordings of the spontaneous reversed beating.

According to the sliding filament hypothesis, shear angle is proportional to the amount of sliding displacement (u) between peripheral doublet-microtubules. The parallel shift of a portion of shear curves within a fraction of time (Δt) indicates that the rate of sliding displacement ($\Delta u/\Delta t$) is constant within the region that is covered by this portion: $\Delta u/\Delta t>0$ during the propagation of an E-bend (E-sliding) and $\Delta u/\Delta t<0$ during the propagation of an R-bend (R-sliding). It therefore follows that, in normal beating, the rate of sliding displacement was constant along individual bending regions in either direction. In reversed beating, however, the increment of curvature during the propagation of the R-bend indicates that the rate of R-sliding in reversed beating was lower in the distal part of the R-bends, while E-sliding occurred at a constant rate along the whole length of the bending region.

Fig. 5 shows plots of shear angles as a function of the percentage of the beat period in normal and reversed beating, measured at various distances from the base. This figure indicates that, when normalized to the fraction of the beat period, the local oscillation in both normal and reversed beating shows similar patterns among individual cilia. It also suggests that the mean course in each plot, obtained by moving average (curves in Fig. 5),

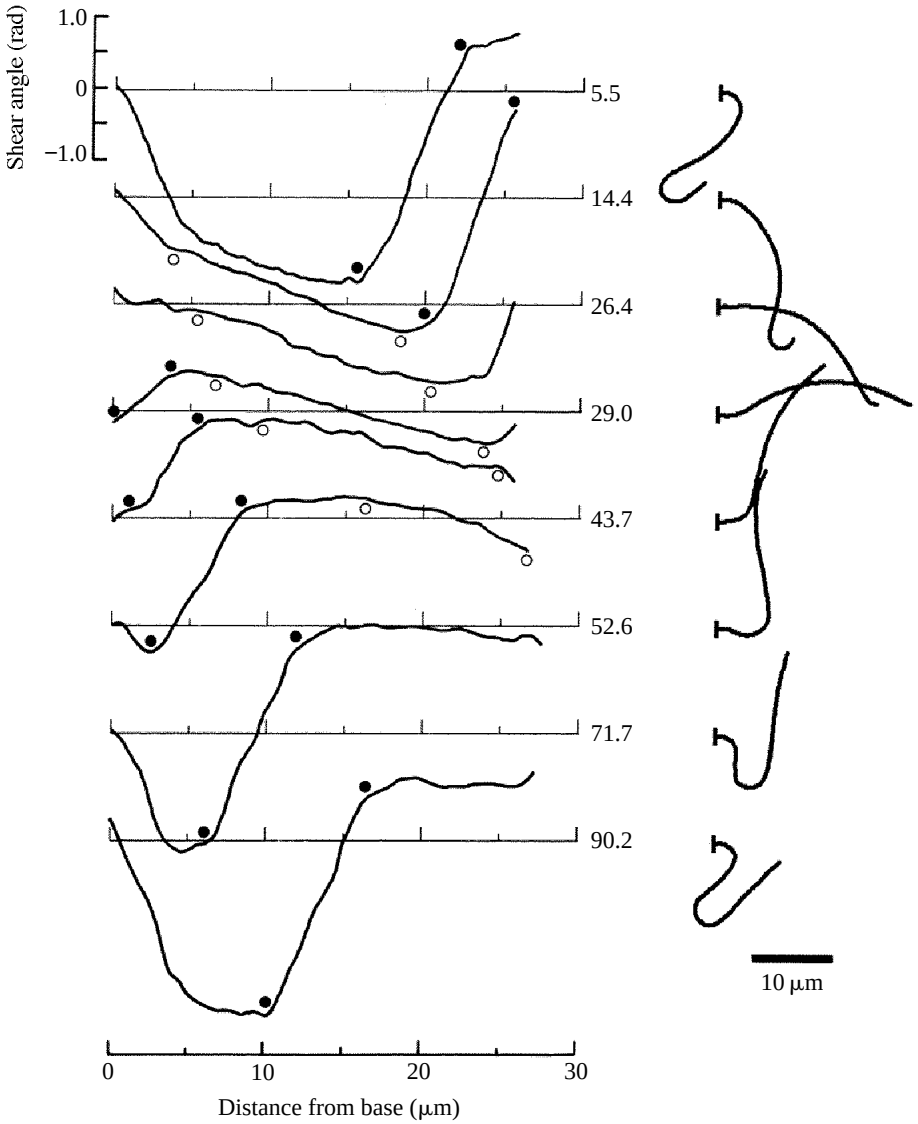

Fig. 3. Shear curves and corresponding bending shapes of the cilium in normal beating. Numbers indicate the percentage of the beat period defined with zero at the beginning of the E-rotation. Open and filled circles mark the regions of propagation of E- and R-bends, respectively.

is a good representation of the oscillatory movement. Fig. 6 shows the parameters of the angular oscillation calculated from the mean course.

The time courses of the angular oscillation of normal and reversed beating appear to be similar at the proximal portion (about 2.6 μm from the base; Fig. 5 bottom), where both patterns possess a period with little sliding activity, before the onset of E-sliding. In reversed beating, the pause appears, with almost equal duration, between R- and

successive E-sliding, irrespective of the position along the length of the cilium, although its temporal position is gradually delayed from base to tip. In normal beating, however, the length of the pause before the onset of E-sliding becomes gradually shorter in the

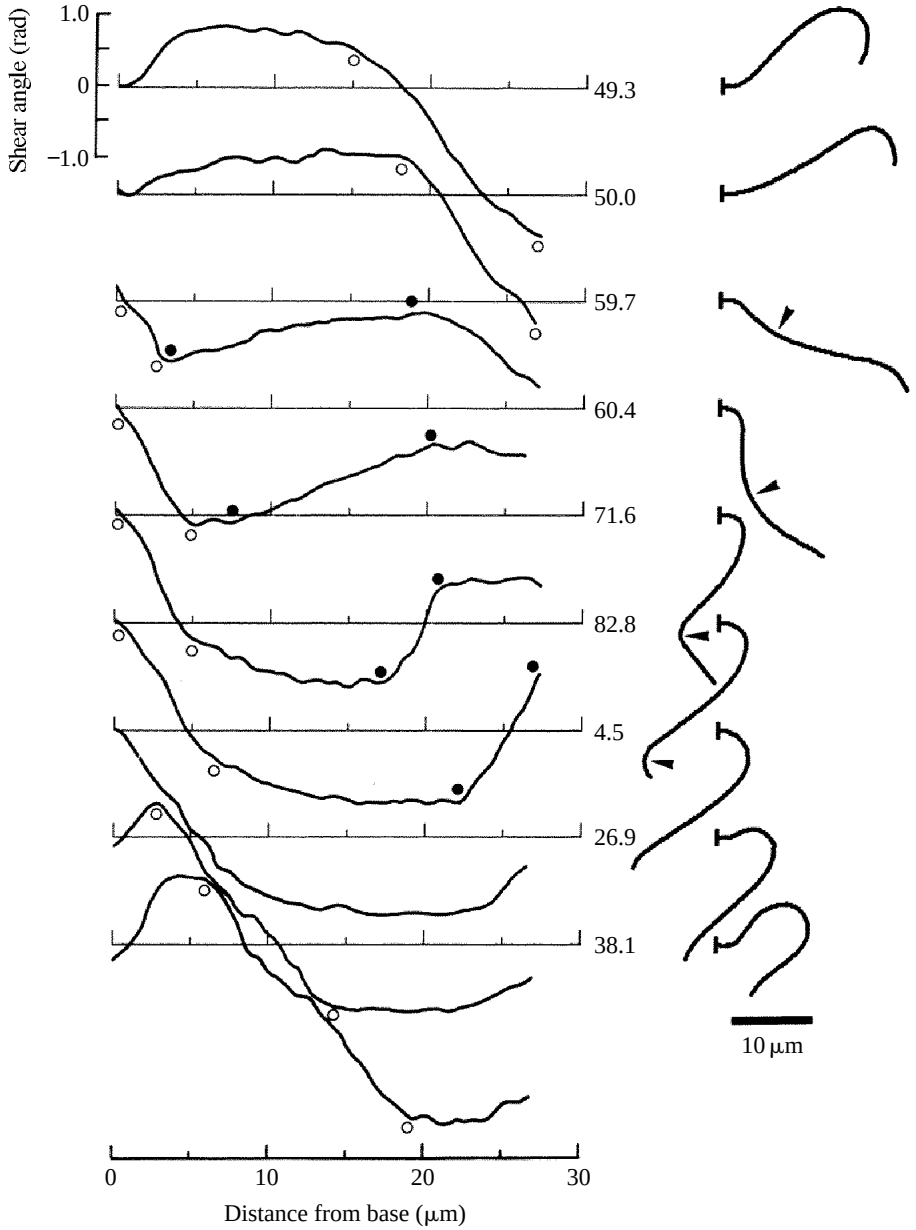

Fig. 4. Shear curves and corresponding bending shapes of the cilium in reversed beating recorded from the cilium shown in Fig. 3. Numbers and symbols have the same meaning as in Fig. 3. Arrowheads in the bending shapes indicate the increasing curvature of the R-bend during propagation.

more distal portions and another pause appears after the end of E-sliding. Fig. 6A shows changes in the temporal pattern of the local oscillation in terms of the fraction of the period between the intersections of the descending limb (R-sliding) and the ascending limb (E-sliding) through the centre line of the oscillation (dashed lines in Fig. 5). The duration of the pause after the end of R-sliding of normal beating gradually decreases towards the tip, so that there appears to be almost a mirror-image relationship at the distal portion between the time courses of the shear angles for normal and reversed beating (Fig. 5, top). Fig. 6B,C indicates that the differences in the amplitudes and in the centre of the oscillation are small in the proximal portion (up to a distance of about 4 μm from the base). In the more distal portion, the amplitude of oscillation of reversed beating is smaller, and the centre of oscillation of reversed beating is more negative than that of the normal beat. The parameters of the local oscillation of normal and reversed beating have almost equal values at the proximal portion, which suggests that the change in bending pattern between normal and reversed beating involves little (or no) change in the oscillatory activity at the base of the cilium.

Discussion

In this paper, ciliary movement was investigated in normal and reversed beating recorded from cells isolated from echinoplutei. Isolation of the cells may change the viscous load on the beating cilium, because the cell body rotates free from the connection to the surface of the embryos. The difference between the hydrodynamic situations of ciliated cells in free rotation and those tethered on the surface of embryos could be compared to that of sperm swimming freely or attached by the head to the substratum. In normal beating, the amplitude of shear angle oscillation at the basal region (2–3 μm from the base) is almost equal in rotating and tethered cells; 0.7–1.5rad in normal beating of rotating cells (Fig. 6B) and about 1.2rad in tethered cells (Baba and Mogami, 1987). In rotating cells, the amplitude increases with the distance from the base, having a maximum at the middle of the cilium, and is attenuated in the more distal region to a smaller value at the tip (0.8–1.1rad) (Fig. 6B) than that measured in tethered cells (about 1.6rad). This may correspond to the constriction of shear amplitude that is observed in the flagellar beating of free-swimming sperm (Brokaw, 1991) but not in sperm attached by the head to the substratum (Hiramoto and Baba, 1978). Changes in the hydrodynamic environment might emphasize the feature of the propagation of the R-bend of reversed beating, with an increase in curvature, which is not very evident when the beat occurs on the tethered cells (Baba and Mogami, 1987).

Rotational movement of the isolated cells can be used as a measure of the water transport by the cilium, as in the case of the rotation of uniflagellated mutant *Chlamydomonas* (Brokaw and Luck, 1983). Since the rotation of the cell occurs under conditions of low Reynolds number (of the order of 10^{-3}), it is inferred that the rotation occurs in close relation to the propulsive thrust exerted by the cilium, which varies within a cycle of beating. Results of the least-squares fitting indicate that the rotational movement caused by normal and reversed beating can be characterized by separate equations. Equation 2 involves a rapid change in the direction between successive cycles.

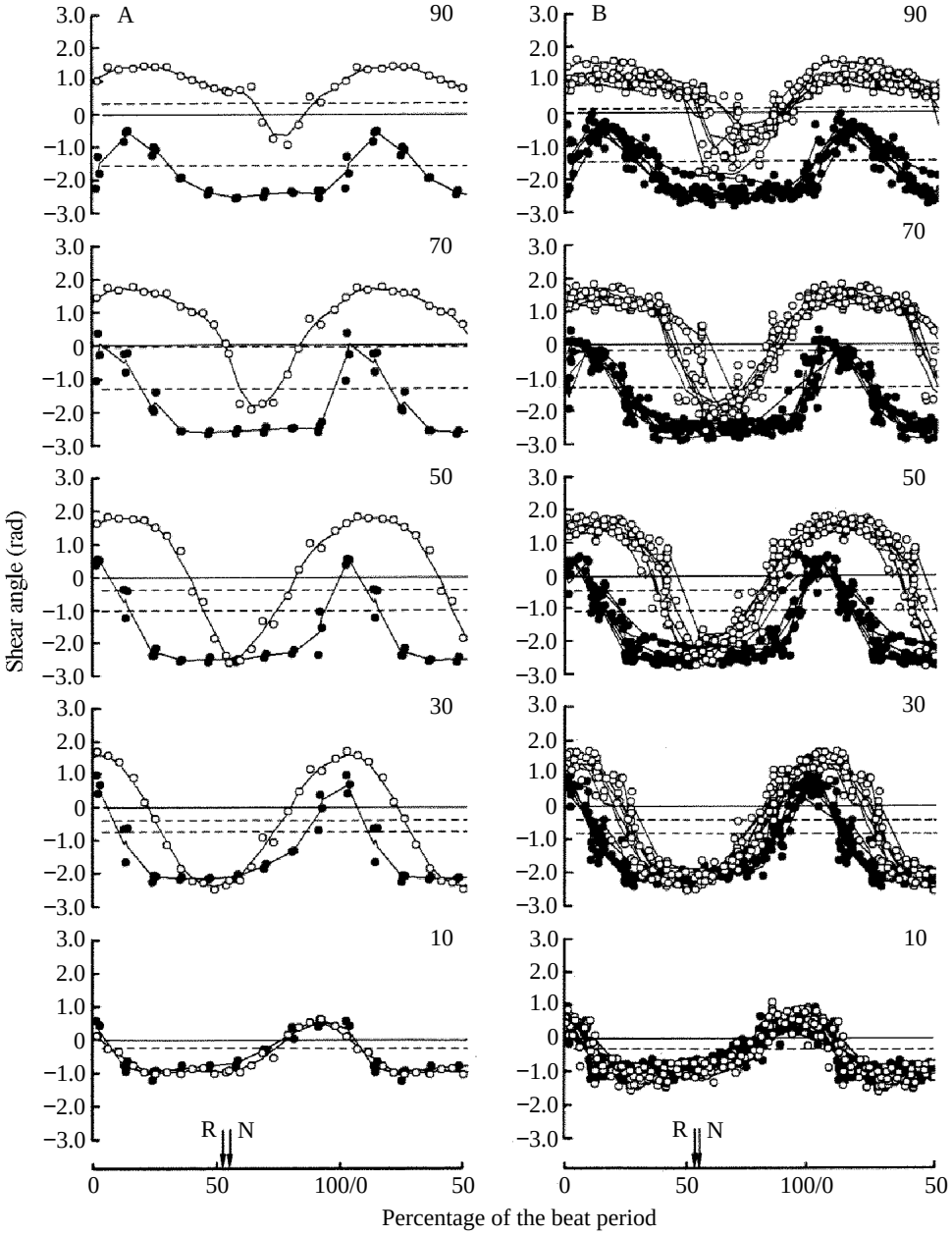

Fig. 5

This may represent the sharp transition between E- and R-rotations in reversed beating, which occurs at the same time as the rapid propagation of E-sliding, followed shortly after by R-sliding (Fig. 5). In normal beating, delays in the onset of R-sliding along the distance from the base (Fig. 5) may result in the gradual transition between E- and R-rotation, as represented by equation 1. The lower value of the mean rotation velocity in

Fig. 5. Time course of the changes in shear angles measured at various distances along the cilium. Shear angles of normal (open circles) and reversed (filled circles) beating are plotted against the percentage of the beat period determined from the rotational movement of the cell body. In A, data from 4.1 cycles of normal and 2.4 cycles of reversed beating of the cell shown in Figs 3 and 4 are plotted with the mean course obtained by moving averages (solid lines). Dashed lines indicate the centre of the oscillation determined on the basis of the mean course. In B, data from 2–15 cycles of normal and 2–13 cycles of reversed beating and the mean courses of each curve (solid lines) obtained from six cells, whose rotational parameters are summarized in Table 1, are superimposed with the centre of each curve shifted to the average values (dashed lines). Numbers on the right indicate the percentage from the base of the full length of each cilium: 26.4 μm for A and 25.8±0.86 μm (24.2–26.5 μm) for B. For ease of direct comparison, the difference of the centre of the oscillation has been subtracted from each curve and the phase of curves has been adjusted to give maximal overlap at the proximal portion. Arrows in A indicate the beginning of E-rotation of normal (N) and reversed beating (R) of the cell and arrows in B indicate the average positions of the cells.

reversed beating (Table 1) suggests that reversed beating has a lower efficiency in water transport than normal beating has. This may explain the lower speed of backward swimming of the plutei (60–80% of the speed of forward swimming) (Degawa *et al.* 1986; Mogami *et al.* 1992). The reduced efficiency seems to be related to symmetrical bend formation in reversed beating compared to highly asymmetrical bend formation in normal beating (Figs 3 and 4).

Analyses of the shear angle of normal- and reversed-beating cilia demonstrate that changes in the doublet-microtubule sliding activity depend on the position along the length of the cilium. This is illustrated in the propagation of the R-bend in reversed beating, which involves differences in sliding rate within a bending region (Fig. 4), and in the temporal pattern of the local angular oscillation (Fig. 5). In normal beating, the oscillation was observed to change its temporal pattern along the length of the cilium, although in reversed beating an almost uniform pattern was observed throughout the length. As a result, the difference in the profiles of beating oscillation between normal and reversed beating was greater towards the tip, whereas the proximal region maintained a fixed profile irrespective of the beating pattern. This suggests that the change in bending pattern between normal and reversed beating does not involve changes in the initiation of oscillation activity at the base, but is entirely caused by modification of the propagation of the activity.

Baba and Mogami (1987) previously reported a tipward propagation of the local response at the transient, from normal to reversed beating, that was induced by electrical stimulation. The apparent change at the proximal region during the transition is not necessarily inconsistent with the present data, which show a nearly identical temporal profile of the proximal oscillation for both normal and reversed beating, bearing in mind that the transient response includes a phase shift of oscillatory activity. The time course of the response (Fig. 4 in Baba and Mogami, 1987) can be interpreted as a consequence of the resetting of local oscillatory movement at each point of the cilium to the beginning of E-sliding of the subsequent reversed beating. Provided that the resetting of the oscillation is delayed increasingly towards the tip, a phase shift resulting from the resetting may be observed as the tipward propagation of the local response upon electrical stimulation.

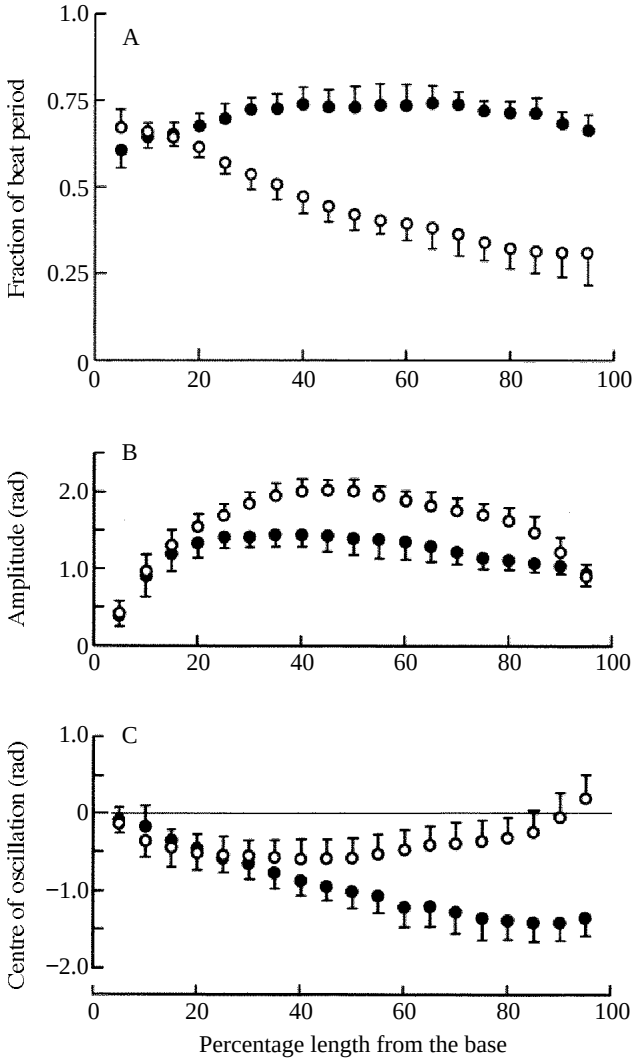

Fig. 6. Parameters of shear angle oscillation as a function of the distance from the base. Observed values (mean ± S.D.) obtained from normal (open circle) and reversed (filled circle) beating of the cells shown in Fig. 5B are plotted as a function of the fraction of the total length (25.8±0.86 μm; 24.2–26.5 μm). (A) Plots of the fraction of the beat period of the time measured from the intersection at the centre of rotation of the ascending limb to that of the descending limb of the mean course of angular changes. (B) Amplitude of the shear angle oscillation. (C) Centre of the shear angle oscillation.

For the regulation of asymmetry of the 'flagellar' beating of sperm and *Chlamydomonas*, Eshel and Brokaw (1987) proposed the biased baseline model. The model explains the change in the beating asymmetry solely by the change in the centre of the oscillation (static bias) on which a symmetrical metachronous oscillation is superimposed. The present data, however, show that, in the transformation of the bending pattern from normal to reversed beating, the change in the static bias occurs

concomitantly with the changes in the temporal pattern of the local oscillation (Fig. 6). Therefore, the change in the bending pattern of sea urchin embryo cilia probably cannot be explained only by an alteration of the centre of oscillation.

From axial view analyses on the basal activity of three-dimensional ciliary beating, Machemer and Sugino (1989) indicated that voltage-activated ciliary responses in *Stylonychia* consisted of static noncyclic and cyclic responses. This fact also suggests that a simple biased baseline model does not apply to the mechanism regulating the beating of the 'ciliary' organelles.

Fig. 6 shows that the difference in the temporal oscillatory activity of the cilium becomes greater in parallel with the increment of the change in the static bias of the oscillation. Do the changes in the two parameters occur independently? Okuno and Brokaw (1981) demonstrated that Ca^{2+} could reversibly change the configuration of a sperm flagellum in the presence of vanadate and ATP. The noncyclic change in the curvature may provide the bias of the propagating metachronous oscillation (Eshel and Brokaw, 1987). In the marginal cirri of *Stylonychia*, voltage-clamp experiments applying extremely slow voltage ramps showed a noncyclic orientation response below the threshold potential of cyclic activity (de Peyer and Machemer, 1973). These results suggest that the mechanism for shifting the spatial bias of oscillations may function independently from the temporal control of the local oscillation. In fact, a 'flip-flop' movement without cyclic activity between two inactive configurations was observed in epaulette cilia of echinoplutei (Mogami *et al.* 1991).

Previous reports suggest that ciliary responses observed in sea urchin embryos are Ca^{2+}-dependent (Baba, 1975; Degawa *et al.* 1986; Baba and Mogami, 1987). The absence of reversed beating in isolated cells immersed in Ca^{2+}-free ASW suggests that an influx of Ca^{2+} into the ciliated cells from the external medium is required for the initiation of reversed beating. Although it is not known whether Ca^{2+} is the primary intracellular regulator of the ciliary beating of sea urchin embryos, the present data indicate that Ca^{2+} would act to regulate the oscillatory activity along the whole length of the cilium.

Reversed beating is performed only after the morphogenesis to pluteus larva. The newly acquired ability to beat in the reversed direction may be needed to alter the ciliary motile apparatus. Detailed analysis of the ciliary beating of the cells isolated from various developmental stages did not show significant differences in the parameters of normal beating, such as the beat frequency, maximum curvature and the rate of E-sliding and the propagation of the R-bend (Sekiguchi *et al.* 1986). This result suggests that incorporation of the capability for reversed beating occurs without affecting the motile mechanism responsible for generating normal beating.

References

BABA, S. A. (1975). Developmental changes in the pattern of ciliary response and the swimming behavior in some invertebrate larvae. In *Swimming and Flying in Nature*, vol. 1 (ed. T. T.-Y. Wu, C. J. Brokaw and C. Brennen), pp. 317–323. New York: Plenum Press.

BABA, S. A. AND MOGAMI, Y. (1985). An approach to digital image analysis of bending shapes of eukaryotic flagella and cilia. *Cell Motility* **5**, 475–489.

BABA, S. A. AND MOGAMI, Y. (1987). High time-resolution analysis of transient bending patterns during

ciliary responses following electric stimulation in sea urchin embryos. *Cell Motility Cytoskel*. **7**, 198–208.

BROKAW, C. J. (1991). Microtubule sliding in swimming sperm flagella: direct and indirect measurements on sea urchin and tunicate spermatozoa. *J. Cell Biol*. **114**, 1201–1215.

BROKAW, C. J. AND KAMIYA, R.(1987). Bending patterns of *Chlamydomonas* flagella. IV. Mutants with defects in inner and outer dynein arms indicate differences in dynein arm function. *Cell Motility Cytoskel*. **8**, 68–75.

BROKAW, C. J. AND LUCK, D. J. L. (1983). Bending patterns of *Chlamydomonas* flagella. I. Wild-type bending patterns. *Cell Motility* **3**, 131–150.

BROKAW, C. J. AND LUCK, D. J. L. (1985). Bending patterns of *Chlamydomonas* flagella. III. A radial spoke head deficient mutant and a central pair deficient mutant. *Cell Motility* **5**, 195–208.

BROKAW, C. J., LUCK, D. J. L. AND HUANG, B. (1982). Analysis of the movement of *Chlamydomonas* flagella: The function of the radial-spoke system is revealed by comparison of wild-type and mutant flagella. *J. Cell Biol.* **92**, 722–732.

DEGAWA, M., MOGAMI, Y. AND BABA, S. A. (1986). Developmental changes in Ca^{2+} sensitivity of sea urchin embryo cilia. *Comp. Biochem. Physiol*. **85**A, 83–90.

DE PEYER, J. E. AND MACHEMER, H. (1983). Threshold activation and dynamic response range of cilia following low rates of membrane polarization under voltage-clamp. *J. comp. Physiol*. **150**, 223–232.

ESHEL, D. AND BROKAW, C. J. (1987). New evidence for a 'biased baseline' mechanism for calcium-regulated asymmetry of flagellar bending. *Cell Motility Cytoskel.* **7**, 160–168.

HIRAMOTO, Y. AND BABA, S. A. (1978). A quantitative analysis of flagellar movement in echinoderm spermatozoa. *J. exp. Biol*. **76**, 85–104.

MACHEMER, H. (1986). Electromotor coupling in cilia. In *Membrane Control of Cellular Activity* (*Fortschritte der Zoologie*, vol. 33) (ed. H. C. Luettgau), pp. 205–250. Stuttgart, New York: Gustav Fischer Verlag.

MACHEMER, H. AND SUGINO, K.(1989). Electrophysiological control of ciliary beating: a basis of motile behavior in ciliated protozoa. *Comp. Biochem. Physiol*. **94**A, 365–374.

MOGAMI, Y., FUJIMA, K. AND BABA, S. A. (1991). Five different states of ciliary activity in the epaulette of echinoplutei. *J. exp. Biol*. **155**, 65–75.

MOGAMI, Y. AND MACHEMER, H. (1991). A novel type of ciliary activity in *Stylonychia*: analysis of potential-coupled motor responses in the transverse cirri. *J. exp. Biol*. **161**, 239–255.

MOGAMI, Y., WATANABE, K., OOSHIMA, C., KAWANO, A. AND BABA, S. A. (1992). Regulation of ciliary movement in sea urchin embryos: dopamine and 5-HT change the swimming behaviour. *Comp. Biochem. Physiol*. **110**C, 251–254.

OKUNO, M. AND BROKAW, C. J. (1981). Calcium-induced change in form of demembranated sea urchin sperm flagella immobilized by vanadate. *Cell Motility* **1**, 349–362.

POWELL, M. J. D. (1965). A method for minimizing a sum of squares of non-linear functions without calculating derivatives. *Computer J*. **7**, 303–307.

SEKIGUCHI, S., MOGAMI, Y. AND BABA, S. A. (1986). A quantitative analysis of ciliary movement using isolated cells of sea urchin embryos. *Zool. Sci*. **3**, 977 (Abstract).

SUGINO, K. AND MACHEMER, H. (1988). The ciliary cycle during hyperpolarization-induced activity: An analysis of axonemal functional parameters. *Cell Motility Cytoskel.* **11**, 275–290.

SUGINO, K. AND MACHEMER, H. (1990). Depolarization-controlled parameters of the ciliary cycle and axonemal function. *Cell Motility Cytoskel.* **16**, 251–265.